

# Photoinduced Ferrimagnetic Systems in Prussian Blue Analogues $C^I_xCo_4[Fe(CN)_6]_y$ ( $C^I =$ Alkali Cation). 1. Conditions to Observe the Phenomenon

Anne Bleuzen,<sup>\*,†</sup> Claire Lomenech,<sup>†</sup> Virginie Escax,<sup>†</sup> Françoise Villain,<sup>†,‡</sup> François Varret,<sup>§</sup> Christophe Cartier dit Moulin,<sup>†,‡</sup> and Michel Verdaguer<sup>\*,†</sup>

Contribution from the Laboratoire de Chimie Inorganique et Matériaux moléculaires, Unité CNRS 7071, Université Pierre et Marie Curie, Bât F 74, 4 place Jussieu, 75252 Paris Cedex 05, France, Laboratoire pour l'Utilisation du Rayonnement Electromagnétique, UMR CNRS 130-CEA-MENRS, Bât 209d, Université Paris-sud, BP34, 91898 Orsay Cedex, France, and Laboratoire de Magnétisme et d'Optique, CNRS-Université de Versailles, UMR 8634, 45 avenue des Etats-Unis, 78035 Versailles Cedex, France

Received January 31, 2000

**Abstract:** Photoinduced magnetization has been recently evidenced by Hashimoto et al. in CoFe Prussian blue analogues. We synthesized three compounds with a variable cobalt environment to point out the conditions required to observe the photoinduced magnetization. Structure and electronic structure of the compounds have been investigated combining XANES, infrared spectroscopy, and powder X-ray diffraction experiments. Magnetization as a function of temperature before and after irradiation showed that diamagnetic pairs  $Co^{III}-NC-Fe^{II}$  are necessary for the existence of the photoinduced magnetization, but their presence is not a sufficient condition. The role of hexacyanoferrate vacancies in the phenomenon is pointed out.

## Introduction

The old Prussian blue analogues have been brought up to date due to their properties as molecule-based magnets.<sup>1–4</sup> Beyond materials with purely magnetic properties, the interest for materials combining magnetic and other properties, among them optical, is growing. In 1996, Hashimoto and co-workers evidenced a new phenomenon in Prussian blue analogues. Starting from aqueous Co(II) and hexacyanoferrate(III), they obtained a powder that exhibits spectacular photoinduced magnetization at low temperature.<sup>5–8</sup> The proposed explanation of the phenomenon was the presence of diamagnetic low-spin Co(III)–Fe(II) pairs in the compound and a photoinduced electron transfer from Fe(II) to Co(III) through the cyanide bridge to produce  $Co^{II}-Fe^{III}$  magnetic pairs.<sup>5,9,10</sup> We undertook a study of the phenomenon in systems where the amount and

nature of the alkali cation have been varied. We report our main results in three parts. In part 1, we correlate the quantity of diamagnetic pairs in the compounds to the efficiency of the photoinduced magnetization. In part 2, we study the electronic structure as well as the local structure around cobalt of the photoinduced metastable state. In part 3, we synthesize a series of compounds in which we precisely control the ligand field around cobalt and the number of hexacyanoferrate vacancies in the structure to correlate them to the efficiency of the photoinduced magnetization.

The synthesis of the powdered samples involves substitution reactions of the water molecules of the hexaqua complex  $[Co^{II}-(H_2O)_6]^{2+}$  by  $[Fe^{III}(CN)_6]^{3-}$ . This means a progressive increase of the Co ligand field as oxygen atoms from water are replaced by nitrogen atoms from cyanides. For a sufficient number of nitrogen atoms around the Co ion, the cobalt ion becomes low spin and its reducing power is strongly enhanced. Then, a chemically induced electron transfer leads spontaneously to a more stable Co(III)–Fe(II) pair. This is a well-known redox process in inorganic chemistry. To increase the number of diamagnetic pairs responsible for the photoinduced effect, one has then to increase the number of nitrogen atoms around the cobalt ion. Once the diamagnetic pairs are obtained, the photoinduced electron transfer should occur, leading to two hypothetical excited states: low-spin or high-spin Co(II)–low-spin Fe(III). In any case, Fe(III) surrounded by 6-C bonded cyanides is low spin.

It is well-known in the chemistry of Prussian blue analogues that when using a divalent cation  $A^{II}$  and an hexacyanometalate bearing three negative charges, two extreme stoichiometries may be obtained, according to the electroneutrality of the solid. A lacunary structure  $A^{II}_3[B^{III}(CN)_6]_2 \cdot nH_2O$  is commonly obtained, where the  $[B(CN)_6]$  vacancies are filled by water molecules, coordinated to the  $A^{II}$  cation or zeolitic.<sup>5–7</sup> Using an excess of

<sup>†</sup> Université Pierre et Marie Curie.

<sup>‡</sup> Université Paris-sud.

<sup>§</sup> CNRS-Université de Versailles.

(1) Mallah, T.; Thiebaut, S.; Verdaguer, M.; Veillet, P. *Science* **1993**, *262*, 1554–1557.

(2) William, R. E.; Girolami, G. S. *Science* **1995**, *268*, 397–400.

(3) Ferlay, S.; Mallah, T.; Ouahès, R.; Veillet, P.; Verdaguer, M. *Nature* **1995**, *378*, 701–702.

(4) Holmes, S. M.; Girolami, G. S. *J. Am. Chem. Soc.* **1999**, *121*, 5593–5594.

(5) Sato, O.; Iyoda, T.; Fujishima, A.; Hashimoto, K. *Science* **1996**, *272*, 704–705.

(6) Sato, O.; Einaga, Y.; Iyoda, T.; Fujishima, A.; Hashimoto, K. *J. Electrochem. Soc.* **1997**, *144*, L11–L13.

(7) Sato, O.; Einaga, Y.; Iyoda, T.; Fujishima, A.; Hashimoto, K. *J. Phys. Chem. B* **1997**, *101*, 3903–3905.

(8) (a) Einaga, Y.; Ohkoshi, S.-I.; Sato, O.; Fujishima, A.; Hashimoto, K. *Chem. Lett.* **1998**, 585–586. (b) Sato, O.; Einaga, Y.; Fujishima, A.; Hashimoto, K. *Inorg. Chem.* **1999**, *38*, 4405–4412.

(9) Verdaguer, M. *Science* **1996**, *272*, 698–699.

(10) Bleuzen, A.; Lomenech, C.; Dolbecq, A.; Villain, F.; Goujon, A.; Roubeau, O.; Nogues, M.; Varret, F.; Baudelet, F.; Dartyge, E.; Giorgetti, C.; Gallet, J. J.; Cartier dit Moulin, C.; Verdaguer, M. *Mol. Cryst. Liq. Cryst.* **1999**, *335*, 965–974.

**Table 1.** Microanalysis Results and Proposed Formula for Compounds **1**, **2**, and **3**

sample	C	Co	Fe	C	N	H	O
<b>1</b>	K						
% exptl (calcd)	0.44 (0.34)	19.66 (20.24)	12.97 (13.42)	17.54 (17.32)	20.43 (20.21)	3.07 (3.16)	25.89 (25.30)
	proposed formula: $K_{0.1}Co_4[Fe(CN)_6]_{2.7} \cdot 18.4H_2O$						
<b>2</b>	Rb						
% exptl (calcd)	11.47 (11.57)	17.17 (17.71)	13.25 (13.84)	18.07 (17.87)	20.44 (20.85)	1.89 (1.96)	16.98 (15.64)
	proposed formula: $Rb_{1.8}Co_4[Fe(CN)_6]_{3.3} \cdot 13H_2O$						
<b>3</b>	Cs						
% exptl (calcd)	29.58 (29.00)	13.30 (13.03)	12.04 (11.88)	15.59 (15.33)	18.42 (17.88)	1.47 (1.44)	9.59 (11.43)
	proposed formula: $Cs_{3.9}Co_4[Fe(CN)_6]_{3.9} \cdot 12.9H_2O$						

alkali cation leads to a perfect face cubic centered (fcc) structure  $C^IA^II[B^III(CN)_6]$  in which the  $C^I$  alkali cation occupies half of the interstitial tetrahedral sites.<sup>1,11,12</sup> In intermediate cases, the divalent cation occupies all the fcc sites whereas the occupation of the octahedral sites by the hexacyanometalate varies from 67 to 100% as a function of the amount of alkali cation in the structure. In one unit cell, the number of divalent cations is then always four and the number of hexacyanometalate and alkali cations is equal to  $y$  and  $3y - 8$ , respectively, due to the electroneutrality of the solid. In the following, the formulas will be given as  $C^I_{3y-8}A^II_4[B^III(CN)_6]_y$ .

By introducing various quantities of alkali cations in the structure, we have synthesized three CoFe Prussian blue analogues in which the environment of the cobalt atoms varies from an average of four nitrogen and two oxygen atoms  $CoN_4O_2$  in the lacunary structure  $A^II_4[B^III(CN)_6]_{8/3}$ , to six nitrogen atoms  $CoN_6$  in the compact structure  $C^I_4A^II_4[B^III(CN)_6]_4$  with alkali cations. Their structure and electronic structure have been characterized and correlated to their magnetic properties before and after irradiation.<sup>13</sup>

## Experimental Section

**Materials and Sample Preparation.** Potassium hexacyanoferrate(III) (Fluka, puriss. p.a.), cobalt(II) nitrate (Fluka, p.a.), rubidium nitrate (Aldrich), and cesium nitrate (Aldrich) were used as received. Compound **1** was synthesized by addition of 400 mL of a  $1.5 \times 10^{-3}$  mol  $L^{-1}$  solution of hexacyanoferrate(III) to 100 mL of a  $10^{-2}$  mol  $L^{-1}$  aqueous solution of cobalt(II) nitrate. To introduce alkali cations into the structure, compounds **2** and **3** were synthesized by addition of 400 mL of a  $2.5 \times 10^{-3}$  mol  $L^{-1}$  solution of cobalt(II) nitrate to 50 mL of a  $2 \times 10^{-2}$  mol  $L^{-1}$  aqueous solution of hexacyanoferrate(III) and  $12.5 \times 10^{-3}$  mol  $L^{-1}$  of rubidium nitrate for compound **2** or  $12.5 \times 10^{-3}$  mol  $L^{-1}$  of cesium nitrate for compound **3**.

For all compounds, the pH of the initial solutions was adjusted to 5 by using diluted  $HNO_3$  aqueous solutions. The addition rate was regulated to last 3 h. The powders were centrifuged, washed three times with distilled water, and allowed to dry in air.

The model compounds for X-ray absorption experiments,  $[Co^{II}(H_2O)_6](NO_3)_2$ ,  $K_3[Co^{III}(CN)_6]$ ,  $K_4[Fe^{II}(CN)_6]$ , and  $K_3[Fe^{III}(CN)_6]$  have been used as received.

**Instrumentation.** Elemental analysis of Co, Fe, C, N, K, H, Rb, or Cs was performed at the analysis facility of the CNRS in Vernaison (the oxygen was assumed to be the only other element and its content was obtained by difference to 100%). For each compound, a chemical formula, taking into account the weight percentage of each element, the electroneutrality, and the chemistry of the systems, is proposed.

(11) Lüdi, A.; Güdel, H. U. *Structure and Bonding*; Springer-Verlag: Berlin, 1973; pp 1–21.

(12) Griebler, W.-D.; Babel, D. Z. *Naturforsch.* **1982**, *37b*, 832–837.

(13) This paper is an expanded and detailed account of preliminary results presented in ICMM'98 and published as ref 10 and was ready for publication when the paper by Sato et al., who apparently were not aware of our own work, appeared on similar compounds studied with different techniques and leading to similar conclusions (ref 8b).

The error in the coefficients is of the order of magnitude of 0.1. Given the error bars in the coefficient, the formulas are neutral.

Infrared spectra of the powders dispersed in Nujol were recorded at room temperature, over the range  $4000\text{--}400\text{ cm}^{-1}$ , with a Fourier transform spectrometer (Bio-Rad FTS 165).

X-ray absorption near edge spectroscopy (XANES) measurements were performed at the Co and Fe K edges in transmission mode on the XAS 13 beam line at the French synchrotron facility DCI at LURE (Orsay), using an Si 311 double monochromator. The energy calibration was checked by recording simultaneously the spectra of the samples and Co or Fe foils, using a three ionization chambers recording mode. The edge energies of the Co at 7709 eV and the Fe at 7712 eV were fixed at the first inflection point of the metallic foils. Samples were ground and homogeneously dispersed in cellulose pellet. XANES spectra were recorded in a 0.3 eV step size and normalized at the middle of the first EXAFS oscillation.

Powder X-ray diffraction patterns (Co  $K\alpha$ ) were collected with a Philips diffractometer. All diagrams were recorded over the  $5\text{--}40^\circ$  range with steps of  $0.01^\circ$ . Magnetization measurements were performed in a SQUID magnetometer (Quantum Device MPMS5) operating in the alternative mode, equipped with an optical fiber made of multiwire silica. The fiber was connected to a broadband source of light (tungsten halogen lamp, 100 W), through interferential filters (100 nm bandwidth). A cutoff filter provided a large intensity in the range  $750 \pm 50\text{ nm}$ . The energy flux received by the sample was typically  $P = 60\text{ mW cm}^{-2}$ . The magnetization of 3 mg of each sample was measured as a function of the temperature over the range  $5\text{--}25\text{ K}$ . Each compound was then irradiated for 2 h at 10 K and the magnetization was measured a second time as a function of the temperature.

## Results and Discussion

**Elemental Analysis.** Chemical formulas of the three compounds are reported in Table 1. The  $Co^{II}\text{--}Fe^{III}$  pairs or  $Co^{III}\text{--}Fe^{II}$  pairs, generated by the internal redox reaction, cannot be differentiated, and the oxidation states of the metal cations are therefore not given.

The insertion percentage of the alkali cation in the structure increases with the size of the cation. Compound **1** contains very few potassium cations. The Fe/Co ratio is the lowest: the structure is of lacunary type  $A^II_4[B^III(CN)_6]_{8/3}$  containing 33% of hexacyanoferrate vacancies. Cobalt atoms are surrounded by an average of four nitrogen atoms and two oxygen atoms. Compound **3** contains the highest quantity of alkali cation. The Fe/Co = 0.975 ratio nearly reaches its maximum value 1. The structure is nearly a perfect fcc structure  $C^I_4A^II_4[B^III(CN)_6]_4$  and contains only 4% of iron vacancies. Cobalt atoms are surrounded by six nitrogen atoms. The stoichiometry of compound **2** is intermediate. The Fe/Co ratio is 0.825 and the structure contains 17.5% of iron vacancies. Cobalt atoms are surrounded by an average of five nitrogen atoms and one oxygen atom.

**X-ray Absorption Spectroscopy.** X-ray Absorption Near Edge Structure (XANES) experiments at the Co (Figure 1) and Fe (Figure 2) K-edges<sup>14,15</sup> were performed to precisely determine

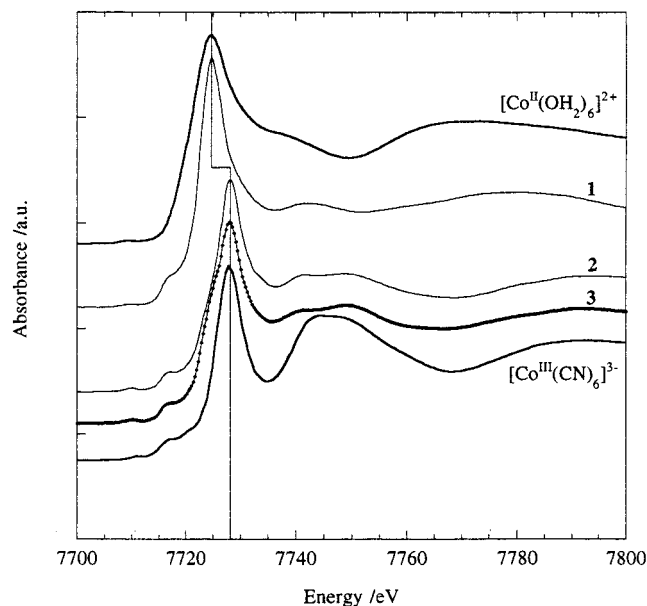


**Figure 1.** Co K-edge XANES spectra of compounds **1**, **2**, and **3** and the model compounds  $[\text{Co}^{\text{II}}(\text{H}_2\text{O})_6](\text{NO}_3)_2$  and  $\text{K}_3[\text{Co}^{\text{III}}(\text{CN})_6]$ .

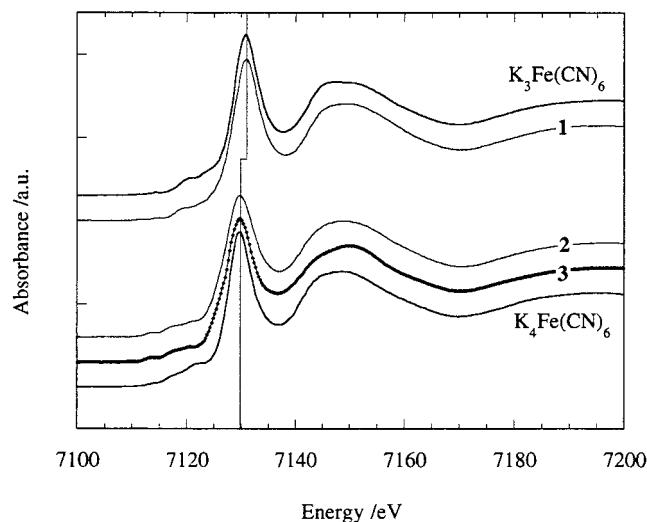


**Figure 2.** Fe K-edge XANES spectra of compounds **1**, **2**, and **3** and the model compounds  $\text{K}_4[\text{Fe}^{\text{II}}(\text{CN})_6]$  and  $\text{K}_3[\text{Fe}^{\text{III}}(\text{CN})_6]$ .

the oxidation states of the iron and cobalt atoms in compounds **1–3** and their spectra were compared to those of the four model compounds  $[\text{Co}^{\text{II}}(\text{H}_2\text{O})_6](\text{NO}_3)_2$ ,  $\text{K}_3[\text{Co}^{\text{III}}(\text{CN})_6]$ ,  $\text{K}_4[\text{Fe}^{\text{II}}(\text{CN})_6]$ , and  $\text{K}_3[\text{Fe}^{\text{III}}(\text{CN})_6]$ .

At the cobalt K edge, Figure 1 presents the spectra of compounds **1–3** and of the model complexes. The spectra present well-resolved features in the beginning of the absorption ramp (7716 eV). These absorption bands are assigned to allowed  $1s (a_{1g}) \rightarrow 3d-\pi^*(\text{CN}) (t_{1u})$  transitions,<sup>16</sup> which shows that the Co ions are linked to CN ligands. The spectrum of compound **1** is very similar to the spectrum of the  $\text{Co}^{\text{II}}$  model (Figure 1). More precisely, the absorption maximum at 7725 eV [allowed  $1s (a_{1g}) \rightarrow 4p (t_{1u})$  transitions] and the weak preedge peak at 7709 eV [forbidden  $1s \rightarrow 3d(t_{2g}, e_g)$  transitions] have the same energies. This similarity indicates that the oxidation state of the

detectable cobalt ions is +II in compound **1**. Given the sensitivity of the technique, the  $\text{Co}^{\text{II}}$  percentage can be considered as close to 100%. The spectra of compounds **2** and **3** are very similar to each other. That means that the local and electronic structures of the cobalt ions are very close. The energies of the absorption maxima are 3 eV shifted to higher energy (7728 eV) compared to the  $\text{Co}^{\text{II}}$  spectrum and fit to the energy of the absorption maximum of the  $\text{Co}^{\text{III}}$  model. This indicates that the oxidation state of the majority of cobalt ions is +III in compounds **2** and **3**. A 1 eV high-energy shift is also observed for the preedge (7710 eV), which confirms the +III oxidation state evidenced with the maximum absorption position. The preedge of the  $\text{Co}^{\text{III}}$  model compound is at higher energy (7711 eV), due to the larger crystal field generated by the carbon atoms of the cyanide ligands. This is not the case in compounds **2** and **3** where the cyanide ligands are N-bonded to the cobalt ions.

Figure 2 shows the iron K-edge spectra of compounds **1–3** compared to the  $\text{Fe}^{\text{II}}$  and  $\text{Fe}^{\text{III}}$  models. All the spectra resemble each other and are characteristic of the  $[\text{Fe}(\text{CN})_6]$  entity.<sup>17</sup> The spectra of compound **1** and  $\text{K}_3[\text{Fe}^{\text{III}}(\text{CN})_6]$  are practically identical. The energy of the weak preedges (7114.5 eV) and of the absorption maxima (7131.0 eV) indicates that the oxidation state of iron ions is +III for the two compounds. The percentage of  $\text{Fe}^{\text{III}}$  ions in **1** can be estimated to 100%.

The spectra of compounds **2**, **3**, and  $\text{K}_4[\text{Fe}^{\text{II}}(\text{CN})_6]$  are very similar. We observe a 1 eV low-energy shift of the preedge and of the absorption maxima compared to the spectrum of compound **1**. This shift is characteristic of the decrease of the oxidation state from +III (compound **1**) to +II (compounds **2** and **3**).

The comparison of the results at the two edges demonstrates that (i) no electron transfer occurs during the synthesis of compound **1**, the oxidation states are those of the precursors, but (ii) on the contrary, an electron transfer occurs from the cobalt to the iron during the synthesis of compounds **2** and **3**, the cobalt is oxidized and the iron reduced.

**Infrared Spectroscopy.** The infrared spectra of compounds **1–3** have been recorded over the  $1900\text{--}2300\text{ cm}^{-1}$  range. The spectrum of compound **1** exhibits three bands. The sharp and intense band at  $2156\text{ cm}^{-1}$  has been attributed to the cyanide stretching vibration mode in the  $\text{Fe}^{\text{III}}\text{--CN--Co}^{\text{II}}$  environment.<sup>18,19</sup> The weak bands at 2118 and  $2090\text{ cm}^{-1}$  have been attributed to the cyanide stretching vibration mode in the  $\text{Fe}^{\text{II}}\text{--CN--Co}^{\text{III}}$  and  $\text{Fe}^{\text{II}}\text{--CN--Co}^{\text{II}}$  environment, respectively.<sup>7</sup> Compound **1** is essentially composed of cobalt atoms at the oxidation state +II and iron atoms at the oxidation state +III, in agreement with the edge spectrum. No electron transfer occurs during the synthesis. Practically no  $\text{Fe}^{\text{II}}\text{--CN--Co}^{\text{III}}$  pairs are then formed.

The spectrum of compound **2** exhibits one broad band centered at  $2125\text{ cm}^{-1}$  with a shoulder at lower energy. This signal can be attributed to the envelope of two main contributions: the stretching of cyanide in the  $\text{Fe}^{\text{II}}\text{--CN--Co}^{\text{III}}$  environment and in the  $\text{Fe}^{\text{II}}\text{--CN--Co}^{\text{II}}$  environment. The displacement of the maximum of intensity is attributable to the overlap of the two signals. Compound **2** contains practically only iron in the oxidation state +II in agreement with iron K-edge. The reduction of the  $\text{Fe}^{\text{III}}$  to  $\text{Fe}^{\text{II}}$ , due to the electron transfer induced by the increasing ligand field around the cobalt during the synthesis, is total. The presence of  $\text{Fe}^{\text{II}}\text{--CN--Co}^{\text{II}}$  is nevertheless

(14) Kulesza, P. J.; Malik, M. A.; Berrettoni, M.; Giorgetti, M.; Zamponi, S.; Schmidt, R.; Marassi, R. *J. Phys. Chem. B* **1998**, *102*, 1870–1876.

(15) Sano, M. *Inorg. Chem.* **1988**, *27*, 4249–4253.

(16) Briois, V.; Cartier, C.; Momenteau, M.; Maillard, P.; Zarembowitch, J.; Dartyge, E.; Fontaine, A.; Tourillon, G.; Thuéry, P.; Verdager, M. *J. Chim. Phys.* **1989**, *86*, 1623–1634.

(17) Yokoyama, T.; Ohta, T.; Sato, O.; Hashimoto, K. *Phys. Rev. B* **1998**, *58*, 8257–8266.

(18) Gadet, V. Thèse, Université Pierre et Marie Curie, Paris, 1992.

(19) Reguera, E.; Bertran, J. F.; Diaz, C.; Blanco, J.; Rondon, S. *Hyperfine Interact.* **1990**, *53*, 391–395.

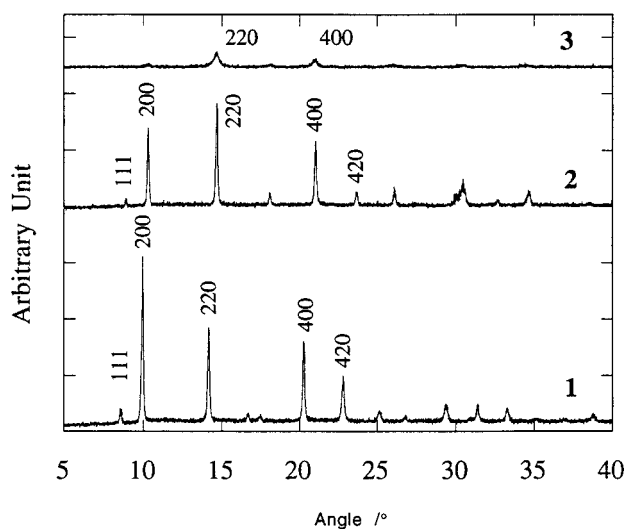


**Figure 3.** X-ray diffraction patterns of compounds **1**, **2**, and **3**.

not surprising. Even if the electron transfer is total, the iron sites are not all filled, so that  $Co^{II}$ -iron vacancy pairs and then  $Fe^{II}$ -CN- $Co^{II}$  bridges are also present. The  $Co^{II}$  signature was not observed by X-ray absorption spectroscopy. So, the percentage of  $Co^{II}$  ions is small. At least the majority of the cobalt atoms are engaged in  $Fe^{II}$ -CN- $Co^{III}$  pairs. The simultaneous presence of  $Co^{III}$  and  $Co^{II}$  in the structure also explains the broadness of the IR bands compared to the bands of compound **1**. The IR spectrum of compound **3** exhibits only one broad band centered at  $2120\text{ cm}^{-1}$ . This is attributable to a majority of  $Fe^{II}$ -CN- $Co^{III}$  pairs. However, the broadness of the band indicates a wide distribution of cyanide entities. In **3**, all the cobalt atoms are at the oxidation state +III. The quantity of  $Fe^{II}$ -CN- $Co^{III}$  pairs reaches its maximum. The broadness of the band indicates a disorder that we attribute to very small crystalline domains, after the X-ray powder diagram.

**X-ray Powder Diffraction.** The powder diffraction patterns of the three compounds are shown in Figure 3. The three diffractograms are characteristic of a face centered cubic structure.<sup>4,20</sup> The diffractogram of compound **1** exhibits intense peaks. As expected for a face cubic centered lattice with cobalt atoms situated at the corners and at the center of the faces of the cube and a partial occupation of the octahedral sites by iron atoms, the reflection 111 is not totally suppressed. The cell parameter has been calculated as  $a = 10.40 \pm 0.05\text{ \AA}$ . For compound **2**, the peaks are still intense. In that compound, the Fe/Co ratio is higher than in **1**, in agreement with a less intense 111 reflection. Furthermore, if a quarter of the tetrahedral interstitial sites is filled with rubidium atoms, the metal atoms and the alkali cations should scatter in phase for the 220 and 400 reflections and out of phase for the 200 and 420 reflections. This is experimentally observed: in compound **2**, the 200 and 420 reflections are less intense, whereas the 400 and 420 reflections are more intense. The calculation of the cell parameters leads to the value of  $10.00 \pm 0.05\text{ \AA}$ , which is clearly smaller than the cell parameter found for compound **1**. This variation reflects a contraction of the cobalt coordination sphere accompanying the oxidation state change from +II in compound **1** to +III in compound **2**. The iron coordination sphere is evidently not concerned because of the well-known similarity of the crystal structures of  $K_4[Fe^{II}(CN)_6]$  ( $d_{Fe-C} = 1.91\text{ \AA}$ ) and  $K_3[Fe^{III}(CN)_6]$  ( $d_{Fe-C} = 1.93\text{ \AA}$ ) entities. The diffraction pattern

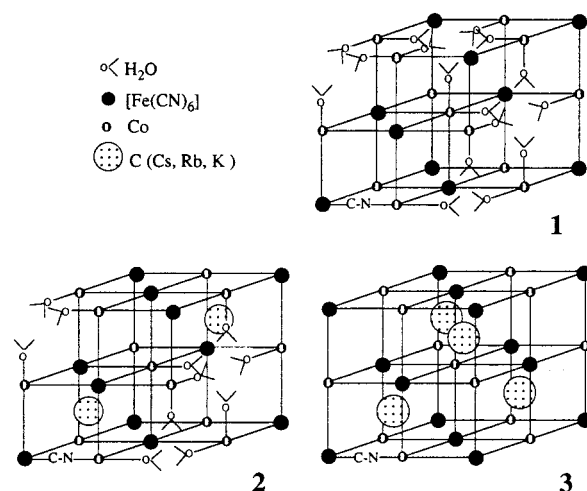


**Figure 4.** Schematic cell representation of compounds **1**, **2**, and **3**. Cyanides (C-bounded to Fe) have been omitted for clarity.

of compound **3** exhibits very weak peaks, which can be related to the absorption of the X-ray radiation by the cesium ion. Furthermore, the peaks broadness can be correlated to the broadness of the infrared band. Scanning electronic microscopy was performed to check that particle size is close in the three compounds in the range of 200–600 nm. The crystalline domains must then be smaller in compound **3**. However, as expected, the 220 and 400 reflections are the more intense. The 200 and 420 reflections are nearly absent due to the destructive interference between the scattering of the metal atoms and the cesium, which occupies half of the interstitial tetrahedral sites, and the nearly complete occupation of the octahedral sites by iron atoms. The 111 reflection is now completely suppressed. In fact, the technique no longer sees the structure as a fcc one, but cubic since the weight of Co and Fe atoms is the same for X-ray diffraction. Since the cobalt ion, ( $t_{2g}$ )<sup>6</sup> is at the oxidation state +III low spin, the  $10.00 \pm 0.05\text{ \AA}$  cell parameter is not surprising.

A schematic representative unit cell of each compound is represented in Figure 4.

**Magnetization Measurements.** Magnetization as a function of temperature before and after irradiation for compounds **1–3** is shown in Figure 5. Compound **1** is ferrimagnetic before irradiation with a  $T_c$  at 16 K.<sup>18</sup> Magnetization exhibits no effect from light. This is not surprising since **1** is built of  $Fe^{III}$ -CN- $Co^{II}$  magnetic pairs. Compound **2** is essentially diamagnetic before irradiation. The compound is built of a majority of diamagnetic  $Fe^{II}$ -CN- $Co^{III}$  pairs where the two  $d^6$  ions are low spin ( $t_{2g}$ )<sup>6</sup>. After irradiation, an important photoinduced magnetization appears. The magnetization is multiplied by 10. The curve obtained after irradiation resembles that of compound **1** with a higher  $T_c$  at  $\approx 21\text{ K}$ .<sup>21</sup> At 5 K, the magnetization of compound **2** after irradiation represents about 50% of the magnetization of compound **1**, which is totally composed of magnetic pairs. Compound **3**, also diamagnetic before irradiation, exhibits only a very small photoinduced magnetization. At 5 K after irradiation, its magnetization represents only 0.25% of the magnetization of compound **1**.

## Discussion and Conclusion

To evidence the efficiency of the photoinduced magnetization as a function of the ligand field around the cobalt ions and the

(20) Yamada, S.; Kuwabara, K.; Koumoto, K. *Mater. Sci. Eng. B* **1997**, *B49*, 89–94.

(21) Varret, F.; Constant-Machado, H.; Dormann, J. L.; Goujon, A.; Jéffit, J.; Noguès, M.; Bousseksou, A.; Klokishner, S.; Dolbecq, A.; Verdager, M. *Hyperfine Interact.* **1998**, *113*, 37–46.

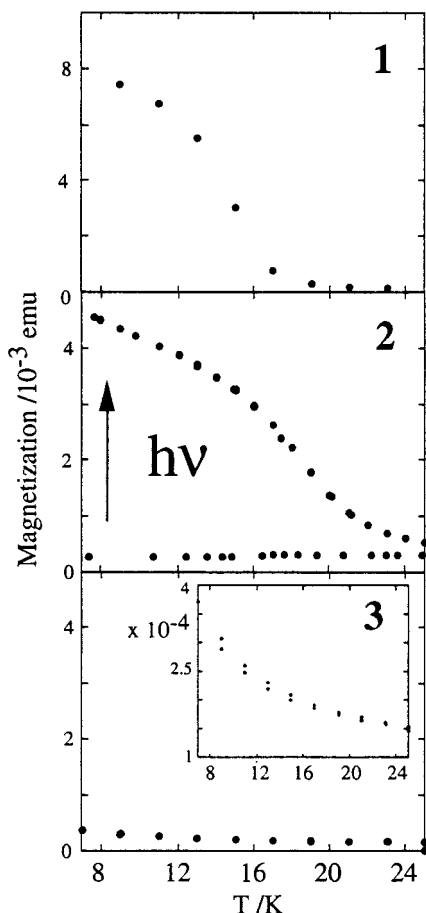


**Figure 5.** Magnetization before and after irradiation as a function of temperature of compounds **1**, **2**, and **3**.

quantity of diamagnetic pairs, we have synthesized three CoFe Prussian blue analogues varying the cobalt atom environment.

Compound **1**, formulated as  $\text{K}_{0.1}\text{Co}^{\text{II}}_4[\text{Fe}^{\text{III}}(\text{CN})_6]_{2.7} \cdot 18.4\text{H}_2\text{O}$ , contains only very few alkaline cations. It is composed of 67%  $\text{Fe}^{\text{III}}-\text{CN}-\text{Co}^{\text{II}}$  pairs. The iron sites are partly occupied. The iron vacancies represent 33% of the sites. The average coordination shell of  $\text{Co}^{\text{II}}$  ions is  $\text{Co}(\text{NC})_4(\text{OH}_2)_2$ . Four  $-\text{NC}$  neighbors around the cobalt ion are not enough to produce a large enough ligand field to favor the low spin configuration of the cobalt and the chemically induced electron transfer leading to the diamagnetic pairs. Compound **1** is mainly made of paramagnetic  $\text{Fe}^{\text{III}}-\text{CN}-\text{Co}^{\text{II}}$  pairs and is ferrimagnetic under 16 K before irradiation. The light has no effect on the magnetization. This fact demonstrates that, as expected, the presence of diamagnetic pairs is necessary to observe a photoinduced magnetization.

Compound **2**, which can be formulated  $\text{Rb}_{1.8}\text{Co}^{\text{III}}_{3.3}\text{Co}^{\text{II}}_{0.7}[\text{Fe}^{\text{II}}(\text{CN})_6]_{3.3} \cdot 13\text{H}_2\text{O}$ , contains 82.5% of diamagnetic pairs  $\text{Fe}^{\text{II}}-\text{CN}-\text{Co}^{\text{III}}$ . The iron sites are not totally filled since the structure still contains 17.5% of iron vacancies. An average of five nitrogen atoms and one oxygen atom here surround the cobalt ions. The enhancement of the ligand field produced by this environment appears sufficient to induce the redox reaction leading to the diamagnetic pairs. As expected, compound **2** is nearly diamagnetic before irradiation. The magnetization at 5 K is multiplied by 10 under irradiation with a Curie temperature at 21 K. The ratio of the number of magnetic neighbors in compounds **1** and **2** ( $4/5 = 0.8$ ) is very close to the ratio of the Curie temperatures ( $16/21 = 0.76$ ). This is an amazingly simple

confirmation of the molecular field approach proposed by Néel for three-dimensional ferrimagnets:  $T_c$  is proportional to  $|J|$ , the absolute value of the coupling constant, and  $Z$ , the number of magnetic neighbors.<sup>1,22</sup> The result indicates with a strong presumption that  $J$  is the same in both compounds and that the magnetic pairs already present in compound **1** (high-spin  $\text{Co}^{\text{II}}-\text{low-spin Fe}^{\text{III}}$ ) are similar to those created under irradiation in compound **2**. Even if this point necessitates further experimental demonstration anyway, such values of the Curie temperature and of the magnetization mean that compound **2** after irradiation is not composed of isolated magnetic pairs, but of three-dimensional magnetic domains, with an efficient percolation between the exchange-coupled pairs.

Compound **3**, formulated  $\text{Cs}_{3.9}\text{Co}^{\text{III}}_4[\text{Fe}^{\text{II}}(\text{CN})_6]_{3.9} \cdot 12.9\text{H}_2\text{O}$ , is composed of a maximum of diamagnetic pairs  $\text{Fe}^{\text{II}}-\text{NC}-\text{Co}^{\text{III}}$  in our series. It is nearly a perfect fcc structure with cesium cations in half of the tetrahedral sites. As expected it is diamagnetic before irradiation. The effect of light is very weak and at a first glance the result is surprising. The behavior of compound **1** shows clearly that the presence of diamagnetic pairs in the compound is compulsory to observe a photoinduced magnetization. At the opposite end, the behavior of compound **3** clearly evidences that it is not a sufficient condition. The phenomenon apparently disappears when too many diamagnetic pairs are present. To explain the result, we propose the following hypothesis. The photoinduced electron transfer implies a change of the cobalt oxidation state from low-spin  $\text{Co}^{\text{III}}$ , with no electron in the antibonding  $e_g^*$  orbitals, to low-spin or high-spin  $\text{Co}^{\text{II}}$ , with respectively one and two electrons in the antibonding  $e_g^*$  orbital. The photoinduced electron transfer should then be accompanied by an increase of the bond lengths in the coordination sphere of the cobalt by 0.15 to 0.20 Å according to published values in cobalt complexes.<sup>23</sup> To be able to absorb the dilatation of the  $\text{Co}-\text{N}$  distance and the related increase of the cell parameter, the inorganic network needs to be flexible. The iron vacancies are filled with water molecules coordinated to the cobalt(II) and loosely hydrogen bonded to other water molecules and behave as relaxation points of the network strains. In compound **3**, the relaxation sites are absent, the framework is more rigid, so that the excited state never reaches its equilibrium distance and relaxes immediately.

The verification of this hypothesis goes through the study of the electronic structure as well as the local structure around the cobalt in the photoinduced excited state. Compound **2**, which proved a very efficient photomagnet, has then been chosen for such a study which is described in part 2.<sup>24</sup>

**Acknowledgment.** We thank A. Goujon and O. Roubeau for the magnetic measurements and the European Community (Grant ERBFMRXCT980181) and CNRS (Program Matériaux) for financial support.

**Supporting Information Available:** Infrared spectra of compounds **1**, **2**, and **3** and scanning electron microscopy images of compounds **1** (a), **2** (b), and **3** (c) (PDF). This material is available free of charge via the Internet at <http://pubs.acs.org>.

JA000348U

(22) Néel, L. *Ann. Phys. Paris* **1948**, *3*, 10–198.

(23) Gallois, B.; Real, J.-A.; Hauw, C.; Zarembowitch, J. *Inorg. Chem.* **1990**, *29*, 1152–1158.

(24) Part 2: Cartier dit Moulin, C.; Villain, F.; Bleuzen, A.; Arrio, M.-A.; Sainctavit, P.; Lomenech, C.; Escax, V.; Baudelet, F.; Dartyge, E.; Gallet, J.-J.; Verdagner, M. *J. Am. Chem. Soc.* **2000**, *122*, 6653–6658.